

ARL-TR-8989 • JULY 2020



Co-Cultures of Neurons and Astrocytes: Alterations to Morphology and Cell-Type Distribution

by Erika A Matheis, Amy J Wegener, Meaghan Richardson, and
Ann Mae DiLeonardi

Approved for public release; distribution is unlimited.



NOTICES

Disclaimers

The research reported in this document was performed in connection with contract/instrument W911QX-16-D-0014 with the US Army Combat Capabilities Development Command (CCDC) Army Research Laboratory (ARL). The views and conclusions contained in this document are those of the authors and should not be interpreted as presenting the official policies or position, either expressed or implied, of the CCDC ARL or the US government unless so designated by other authorized documents. Citation of manufacturer's or trade names does not constitute an official endorsement or approval of the use thereof. The US government is authorized to reproduce and distribute reprints for government purposes notwithstanding any copyright notation hereon.



Co-Cultures of Neurons and Astrocytes: Alterations to Morphology and Cell-Type Distribution

Erika A Matheis

Bennett Aerospace Inc

Amy J Wegener and Ann Mae DiLeonardi

Weapons and Materials Research Directorate, CCDC Army Research Laboratory

Meaghan Richardson

Oak Ridge Associated Universities

REPORT DOCUMENTATION PAGE

Form Approved
OMB No. 0704-0188

Public reporting burden for this collection of information is estimated to average 1 hour per response, including the time for reviewing instructions, searching existing data sources, gathering and maintaining the data needed, and completing and reviewing the collection information. Send comments regarding this burden estimate or any other aspect of this collection of information, including suggestions for reducing the burden, to Department of Defense, Washington Headquarters Services, Directorate for Information Operations and Reports (0704-0188), 1215 Jefferson Davis Highway, Suite 1204, Arlington, VA 22202-4302. Respondents should be aware that notwithstanding any other provision of law, no person shall be subject to any penalty for failing to comply with a collection of information if it does not display a currently valid OMB control number.

PLEASE DO NOT RETURN YOUR FORM TO THE ABOVE ADDRESS.

1. REPORT DATE (DD-MM-YYYY) July 2020		2. REPORT TYPE Technical Report		3. DATES COVERED (From - To) November 2017–August 2019	
4. TITLE AND SUBTITLE Co-Cultures of Neurons and Astrocytes: Alterations to Morphology and Cell-Type Distribution				5a. CONTRACT NUMBER	
				5b. GRANT NUMBER	
				5c. PROGRAM ELEMENT NUMBER	
6. AUTHOR(S) Erika A Matheis, Amy J Wegener, Meaghan Richardson, and Ann Mae DiLeonardi				5d. PROJECT NUMBER	
				5e. TASK NUMBER	
				5f. WORK UNIT NUMBER	
7. PERFORMING ORGANIZATION NAME(S) AND ADDRESS(ES) CCDC Army Research Laboratory ATTN: FCDD-RLW-PB Aberdeen Proving Ground, MD 21005				8. PERFORMING ORGANIZATION REPORT NUMBER ARL-TR-8989	
9. SPONSORING/MONITORING AGENCY NAME(S) AND ADDRESS(ES)				10. SPONSOR/MONITOR'S ACRONYM(S)	
				11. SPONSOR/MONITOR'S REPORT NUMBER(S)	
12. DISTRIBUTION/AVAILABILITY STATEMENT Approved for public release; distribution is unlimited.					
13. SUPPLEMENTARY NOTES ORCID ID(s): Ann Mae DiLeonardi, 0000-0002-1476-7726; Erika A Matheis, 0000-0002-5122-1503					
14. ABSTRACT The brain is possibly the most complicated organ in the body, making understanding its function in normal or pathological states difficult. In vitro models using brain cells reduce some complexity and offer a high degree of experimental control compared with in vivo experiments. Many in vitro models include only neurons in culture, but neurons are surrounded by glial cells in the brain. Including other cell types in co-culture can dramatically change the response of those cells and is more representative of in vivo conditions but increases culture complexity. The astrocyte-to-neuron ratio can be manipulated via different culturing techniques but is not well characterized. Primary pyramidal neurons from rat hippocampi were cultured to obtain three configurations: confluent astrocyte, sporadic astrocyte, and astrocyte free. Qualitatively, neurons appeared healthier in astrocyte-containing cultures, as indicated by thicker neurites and no evidence of free-floating debris or neurite beading, compared with astrocyte free. Each condition was characterized via astrocyte-to-neuron ratio, neurite length, and branching analysis with significant differences among all groups. The confluent-astrocyte group had the largest astrocyte-to-neuron ratio and the lowest values for neurite length and branching. This study characterized cell cultures under different media conditions to help inform future work.					
15. SUBJECT TERMS cell culture, media characterization, glia, astrocyte, primary neurons					
16. SECURITY CLASSIFICATION OF:			17. LIMITATION OF ABSTRACT UU	18. NUMBER OF PAGES 23	19a. NAME OF RESPONSIBLE PERSON Ann Mae DiLeonardi
a. REPORT Unclassified	b. ABSTRACT Unclassified	c. THIS PAGE Unclassified			19b. TELEPHONE NUMBER (Include area code) (410) 306-0689

Contents

List of Figures	iv
List of Tables	iv
1. Introduction	1
2. Methods	2
2.1 Cell Culture	2
2.2 Neuron Isolation and Dissociations	2
2.3 Media Manipulation	3
2.4 Fixation and Immunocytochemistry	3
2.5 Imaging and Cell Quantification	4
2.6 Image Processing	4
2.7 Data Analysis	6
3. Results	6
3.1 Morphology	6
3.2 Cell-Type Ratio	7
3.3 Sholl Analysis	8
4. Discussion	9
5. Conclusion	11
6. References	12
List of Symbols, Abbreviations, and Acronyms	16
Distribution List	17

List of Figures

Fig. 1	Sholl analysis using FIGI plug-in Simple Neurite Tracer: A) single neuron was selected from each image and traced, path zero selected (green) and analysis performed; B) Sholl image, a density map of number of intersections as function of radius; and C) Sholl profile, the number of intersections as function of radius 5
Fig. 2	Representative 20× images of three conditions: A) and B) astrocyte free, arrows are neuronal cell bodies, arrowheads are punctate; C) and D) confluent astrocyte, arrows are neuronal cell bodies, arrowheads are astrocytes; and E) and F) sporadic astrocyte, arrows are neuronal cell bodies, arrowheads are astrocytes. 7
Fig. 3	All astrocyte conditions were significantly different from each other in astrocyte-to-neuron ratio ($p < 0.01$) where confluent astrocyte had the largest percentage of astrocytes; astrocyte free had the largest percentage of neurons and sporadic astrocyte was close to a 1:1 ratio of astrocyte-to-neuron. 8
Fig. 4	Full Sholl profile graphing average number of intersections as function of distance from cell body for each astrocyte condition; neurons grown on confluent astrocytes had significantly less branching at 48–195 μm (48–145 μm , $**p < 0.01$; 145–195 μm , $*p < 0.05$) 9

List of Tables

Table 1	Quantitative measurements from neurite tracings for the different astrocyte conditions 8
---------	--

1. Introduction

The brain is possibly the most complicated organ in the body, making understanding its function in normal or pathological states difficult. In vitro models of brain cells provide a means to reduce the complexity of the full brain by observing how brain cells respond to various stimuli as well as offer a high degree of experimental control compared with in vivo experiments. Many in vitro models include only neurons in culture, but neurons are surrounded by glial cells in vivo, and in some areas of the brain, glial cells can outnumber neurons 10:1.^{1,2} The concentration of glial cells is not uniform throughout the brain,³ therefore building an in vitro model where the concentration of glial cells can be controlled is important.

There are four types of glial cells present in the central nervous system (CNS): oligodendrocytes (myelin sheath), microglia (immune response), ependymocytes (cerebrospinal fluid production), and astrocytes (homeostasis). Astrocytes are the most abundant type of glial cell and provide homeostasis to the neurons by regulating extracellular concentrations of ions and neurotransmitters available, among many other functions (reviewed by Araque and Navarrete⁴). Astrocytes offer support to neurons via release of trophic factors, important for neuronal growth and repair, and molecules to shape the extracellular matrix, the 3-D network that provides structural and biochemical support to the cells.⁵ In culture, the quality and attachment of neurons improve when astrocytes are present compared with a glass coverslip alone.^{6,7} Following mechanical trauma, astrocytes proliferate and serve as chemical “buffers” to potentially reduce the load on injured neurons.⁸⁻¹¹ Including other cell types in co-culture can dramatically change the response of neurons following mechanical trauma.¹²

Astrocytes can greatly affect the health of neurons; however, astrocytes can be cultured in various ways to support neurons and model the physiological environment. Astrocytes can be grown in culture as a distinct layer to offer support to neurons grown separately.¹³⁻¹⁸ This method is particularly advantageous for low-density neuronal cultures.¹⁷ The astrocyte layer is suspended over neuron cultures to release trophic substances into the medium that enhance the development of neuronal processes, accelerate the presence of electrophysiological activity, and improve neuron viability.¹³⁻¹⁷ Distinct astrocyte and neuron layers are useful in culture to monitor responses of the neurons alone because the two layers are separate. Alternatively, astrocytes and neurons can be co-cultured to better model the physiological environment.¹⁹ This is achieved by adding astrocytes directly to neuron cultures or by culturing the neurons in astrocyte-conditioned

medium. Astrocytes in co-culture promote greater synaptic density, increased electrophysiological response, and better neuron survival.¹⁴

Considering the importance of astrocytes in neuronal health and injury response, investigating the effects of a simplified neuronal co-culture with a single glial cell type (i.e., astrocytes) on the morphological development of pyramidal neurons is beneficial for selecting the most appropriate in vitro model for future neuronal injury studies. Using two methods of in vitro astrocyte inclusion is explored in this study to determine the effect of each configuration on neuronal health and provide recommendations for which configuration is most appropriate for specific applications.

2. Methods

2.1 Cell Culture

Two days prior to culturing neurons, 22- × 22-mm coverslips (Corning, catalog [cat.] no. 2845-22) were placed in a glass dish on gauze pads and covered with aluminum foil. The coverslips were sterilized in an autoclave at 138 °C for 30 min. Once the coverslips cooled, the dish was moved to the biosafety cabinet (BSC) and a single coverslip was placed in each well of sterile Costar 6 well plates (Corning, cat. no. 3736). Poly-L-lysine (PLL; Sigma, cat. no. P1524) was diluted to 0.01 mg/mL by adding 1 mL of stock PLL (1 mg/mL) to 99 mL of sterile water. Working PLL was filter-sterilized by passing the solution through a 0.22- μ M filter, and 3 mL of PLL was added to each well, then left in the BSC with the blower off for 20–24 h. The following day, PLL was removed from the plates using vacuum suction and coverslips were washed with sterile water twice for 10 min. After the second wash, additional sterile water was put on the coverslips and plates were moved to the incubator at 37 °C and 5% CO₂ overnight until culturing the following day.

On the day of the cultures, about 20–24 h after the sterile water washes, the water was removed from the wells using vacuum suction and 1.5 mL of filter-sterilized feeding media (Neurobasal media, Gibco, cat. no. 21103049; 2% B-27, Invitrogen, cat. no. 17504044; and 0.4 mM GlutaMAX, Invitrogen, cat. no. 35050061) was placed in the wells. Plates were returned to the incubator.

2.2 Neuron Isolation and Dissociations

Embryonic day-18 (E18) rat hippocampi (cat. no. SDEHP) were purchased from BrainBits, LLC (Springfield, Illinois). Hippocampi arrived in BrainBits Hibernate

media and were stored at 4 °C for 24 h prior to culturing. When ready to culture, the hippocampi were incubated in 5 mL of feeding media containing trypsin (0.3 mg/mL, Sigma-Aldrich, cat. no. T9935-100mg) and DNase I (0.2 mg/mL, Sigma-Aldrich, cat. no. 10104159001) for 20 min in the incubator at 37 °C. Hippocampi were carefully removed and placed into a clean 15-mL conical tube using a glass Pasteur pipette, and the remaining feeding media with trypsin/DNase I was removed. Next, 3 mL of plating media (feeding media containing 5% heat-inactivated fetal bovine serum; Sigma-Aldrich, cat. no. F4135) was added to the hippocampi.

Hippocampi were dissociated by repeatedly pipetting them up and down in progressively smaller pipettes: 10-mL stereological pipette for 10 reps, then a regular Pasteur pipette for 10 reps and finished with a flame-polished Pasteur pipette (BrainBits cat. no. FPP). Cells were counted on a hemocytometer to determine density. Cells were then plated on the glass coverslips and returned to the incubator. Filter-sterilized, warmed feeding media was replaced 4 days after the initial plating, then 1–2 times per week. Cells were maintained at 37 °C, 5% CO₂ for up to 12 days in vitro (DIV). If a well became infected, it was cleared and excluded from the study.

2.3 Media Manipulation

Three different neurobasal media (NBM) configurations were chosen to provide a range of astrocyte-to-neuron ratio conditions for evaluation:

- Condition 1 (n = 5 wells): Astrocyte-free, NBM–B27–GlutaMAX (ThermoFisher Scientific, Grand Island, New York), where the anti-mitotic agent Cytosine β-D-arabino-furanoside (Ara-C, 1 μM; Sigma, cat. no. C1768) was added 24 h post-plating. Ara-C inhibits mitosis, resulting in little to no astrocyte being present in the culture.
- Condition 2 (n = 6 wells): Sporadic Astrocyte, NbActiv1 (BrainBits), produced neuronal cultures with sporadic astrocyte growth intermingled among neurons.
- Condition 3 (n = 6 wells): Confluent Astrocyte, co-culture media (BrainBits), produced cultures with a bed of confluent astrocytes where neurons grow on top of the confluent astrocytes.

2.4 Fixation and Immunocytochemistry

At DIV 12, cells were incubated with 4% paraformaldehyde for 15 min at room temperature, then washed with cold (4 °C) 1× phosphate-buffered saline (PBS)

three times. For immunocytochemistry, cells were permeabilized with 0.25% Triton X-100 for 10 min and blocked with 10% bovine serum albumin for 30 min. Cultures were incubated with the 1° antibodies (glial fibrillary acid protein [GFAP], a marker for glia and Beta-III Tubulin, a marker for neurites) for 1 h, followed by a 1-h incubation with the 2° antibodies. Cultures were then mounted to slides using Prolong Diamond with 4',6-diamidino-2-phenylindole (DAPI), for visualizing the nuclei.

2.5 Imaging and Cell Quantification

Using a Nikon Eclipse Ti-U inverted microscope (Nikon Instruments Inc, Melville, New York), phase-contrast images (20×) were taken to capture images at DIV 12 and used to determine the ratio of neurons to astrocyte in each of the three conditions. Eight images were captured per well and each image needed a minimum of 10 cells to be included in the analysis (astrocyte free: n = 41 images; confluent astrocyte: n = 24 images; and sporadic astrocyte: n = 41 images). Additionally, for the sporadic and confluent conditions, a minimum of two of each cell type was required to be included in the analysis. Cells were manually counted by an experienced, condition-blinded scientist with 6 years of cell-culture microscopy experience. Cells with phase-bright cell bodies were counted as neurons, and cells with granulated cell bodies were counted as astrocytes. This was qualitatively confirmed by visualization with immunocytochemical markers. Following completion of immunocytochemistry, fluorescent images (20×) were acquired from the neurons fixed at DIV 12. Astrocytes were identified with a GFAP-specific antibody and visualized with a fluorescein-isothiocyanate or FITC filter (green). Neurites were identified with a Beta-III Tubulin-specific antibody visualized with a tetramethylrhodamine-isothiocyanate or TRITC filter (red). DAPI was used to stain nuclei of both cell types and visualized with the DAPI filter (blue).

2.6 Image Processing

Image processing was performed using the FIJI²⁰ plug-in, Simple Neurite Tracer,²¹ to characterize neuronal features such as neuronal bodies, or somas, dendrites, and branching for additional analysis. The program identified and outlined the neuronal dendrites from the microscope images by their tube-like structures, demarcated by changes in brightness and contrast within the image (Fig. 1A). The program allowed the user to confirm the accuracy of the automatic tracing; if not accurate, pathways were manually edited. Once the initial dendrite pathways were captured originating from the soma, the secondary and tertiary branches were selected and categorized.

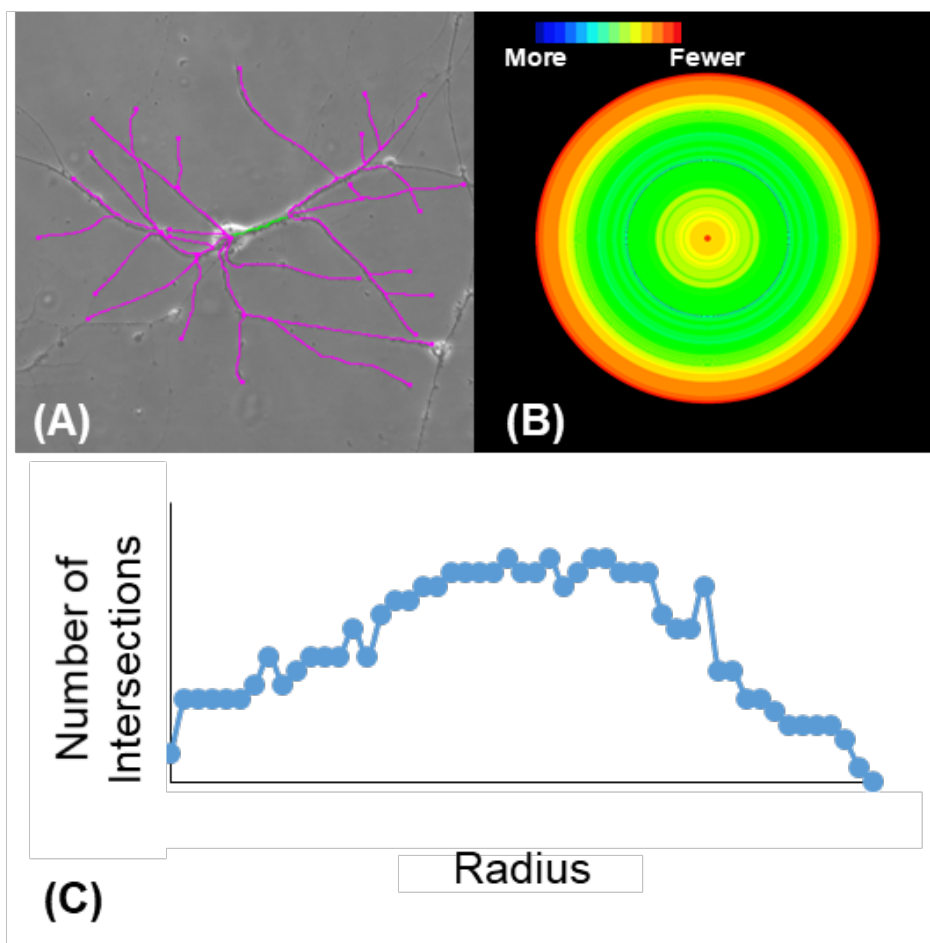


Fig. 1 Sholl analysis using FIGI plug-in Simple Neurite Tracer: A) single neuron was selected from each image and traced, path zero selected (green) and analysis performed; B) Sholl image, a density map of number of intersections as function of radius; and C) Sholl profile, the number of intersections as function of radius

After the somas, dendrites, and branches were identified, additional metrics to describe the neuronal morphology were performed. Neurite length was defined as the length of the longest branch traced from a soma in the initial Simple Neurite Tracer analysis. Branching of neurites was described using the Sholl analysis. The Sholl analysis measures branch intersections, span, and amount of branching through a method of concentric circles starting from the center of the soma and extending outward (Figs. 1A and 1B).²²⁻²⁴ Within Simple Neurite Tracer, the image was converted to an 8-bit luminance format and the center of a single-cell soma was selected from each image. All branches were traced from this starting point using the path feature. The number of branches was plotted as a function of distance from the soma (Fig. 1C). The Simple Neurite Tracer function to fit a polynomial of any degree, up to 8, used a heuristic algorithm to guess a polynomial best-fit.

Other reported values from the Sholl analysis include maximum number of intersections at a concentric circle, maximum intersection radius (radius at which the maximum number of intersections occurs), critical value (the local maximum of intersections in the polynomial fit), and critical radius (distance at which the critical value occurs).

2.7 Data Analysis

Statistical analysis was performed using JMP 14 (SAS Institute Inc., Cary, North Carolina) for cell count, neurite length, and Sholl-analysis data. Averages and standard deviations were calculated for all measurements taken. A one-way analysis of variance (ANOVA) was performed between media conditions. If significance was found at a p-value of less than 0.05 (95% confidence interval) a Tukey HSD* post-hoc analysis was completed to determine the significance between groups.

3. Results

3.1 Morphology

In phase-contrast images, regardless of astrocyte condition, neurons had phase-bright, nongranulated somas (Fig. 2A's arrows) with neurites extending out from the soma. Neurites in astrocyte-free cultures were contiguous; however, they had a punctate appearance and were not smooth (Fig. 2A's arrowheads). Immunoreactivity for Beta-III Tubulin was observed, indicating the presence of neurites, while there was no evidence of GFAP immunoreactivity, demonstrating the lack of astrocytes in these cultures (Fig. 2B). In the confluent astrocyte condition, the astrocytes, confirmed by immunoreactivity for GFAP, cover the entire substrate with phase-bright neurons growing on top (Fig. 2C). The growth of neurons on top of the astrocytes was verified by positive staining for Beta-III tubulin (Fig. 2D). Neurites in this condition were contiguous and lacked the punctated appearance of neurons from the astrocyte-free condition. The final condition resulted in a sporadic distribution of neurons and astrocytes. Neurons can still be identified by their phase-bright somas with contiguous neurites (Fig. 2E's arrows), while somas of astrocytes are granulated and not phase bright (Fig. 2E's arrowheads). Immunoreactivity for GFAP- and Beta-III tubulin-labeled astrocytes and neurons, respectively (Fig. 2E), allowing for the appreciation of the different cell-type morphologies. For example, neurites appeared longer in comparison with

* Honestly Significant Difference

astrocytic branches. Additionally, neurites tapered at their terminals, whereas astrocyte processes branched.

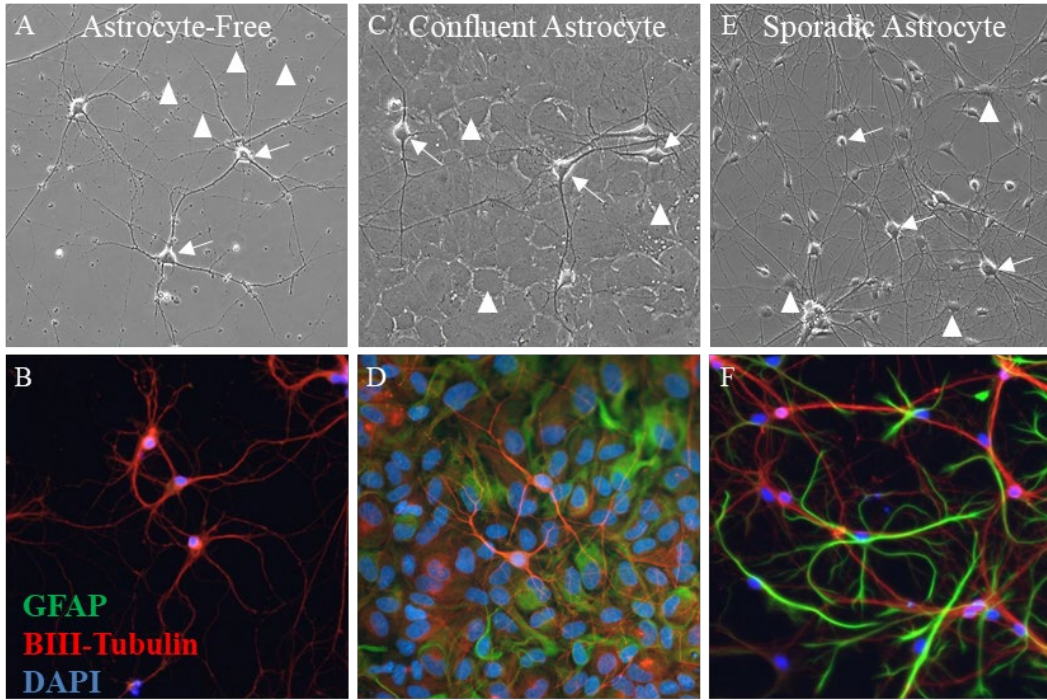


Fig. 2 Representative 20× images of three conditions: **A)** and **B)** astrocyte free, arrows are neuronal cell bodies, arrowheads are punctate; **C)** and **D)** confluent astrocyte, arrows are neuronal cell bodies, arrowheads are astrocytes; and **E)** and **F)** sporadic astrocyte, arrows are neuronal cell bodies, arrowheads are astrocytes.

3.2 Cell-Type Ratio

The numbers of neurons and astrocytes were manually counted to compare the relative amount of each cell type among the different conditions. As expected, the astrocyte-free condition had a ratio of astrocytes-to-neurons of 1:96, with $98.97\% \pm 3.94$ neurons and $1.03\% \pm 3.94$ astrocyte. In the confluent astrocyte condition, the astrocyte-to-neuron ratio was 10:1, with $8.7\% \pm 5.15$ neurons and $91.30\% \pm 5.15$ astrocyte population. The sporadic astrocyte condition had a 1:1 ratio, $45.85\% \pm 23.32\%$ of neurons and $54.15\% \pm 23.32\%$ of astrocytes. The average percent of neurons and astrocytes comprising the cultures was significantly different among all groups (Fig. 3; $p < 0.01$).

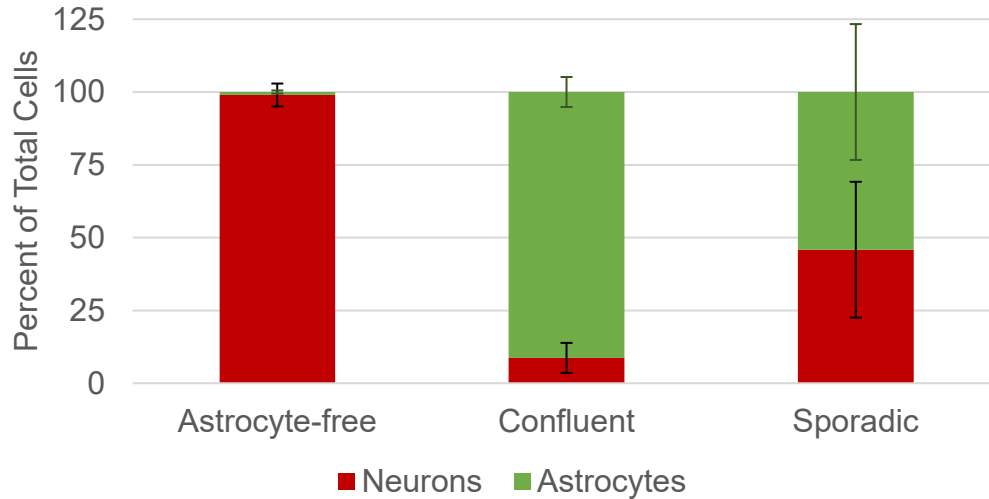


Fig. 3 All astrocyte conditions were significantly different from each other in astrocyte-to-neuron ratio ($p < 0.01$) where confluent astrocyte had the largest percentage of astrocytes; astrocyte free had the largest percentage of neurons and sporadic astrocyte was close to a 1:1 ratio of astrocyte-to-neuron.

3.3 Sholl Analysis

The average Sholl profiles for each astrocyte condition are graphed as the number of intersections plotted as a function of distance from the center of the cell body (Fig. 3). Qualitatively, the profiles show there is a decrease in intersections for the confluent astrocyte condition, suggesting there is less branching of neurites in this condition. The parameters selected for quantitative comparison included neurite length, mean number of intersections, maximum number of intersections, the maximum intersecting radius, the critical value, and the critical radius (Table 1).

Table 1 Quantitative measurements from neurite tracings for the different astrocyte conditions

Measurement	Astrocyte condition		
	Astrocyte free	Sporadic	Confluent
Neurite length (μm)	224.74 \pm 78.15	202.26 \pm 76.76	189.29 \pm 80.23
Mean intersections (N)	8.94 \pm 3.00	8.31 \pm 2.94	5.18 \pm 2.27 ^a
Max intersections (N)	20.56 \pm 6.34	20.67 \pm 9.63	13.55 \pm 6.39 ^a
Max intersecting radius (μm)	68.47 \pm 51.32	58.15 \pm 42.07	53.17 \pm 52.63
Critical value	12.56 \pm 4.29	11.67 \pm 4.19	7.56 \pm 3.58 ^a
Critical radius (μm)	65.32 \pm 34.13	72.58 \pm 45.64	52.75 \pm 50.39

^a $p < 0.01$

A one-way ANOVA, grouped by astrocyte condition, found there was a significant decrease in both mean ($p < 0.01$) and maximum ($p < 0.01$) number of intersections and critical value ($p < 0.01$) for the confluent astrocyte condition compared with

both the sporadic astrocyte and astrocyte-free conditions (Table 1), suggesting neurons grown on a confluent bed of astrocytes branch less than those cultured in the absence of or intermingled with astrocytes. For the full Sholl profiles, there was a significant decrease in intersections between 48 and 195 μm from the center of the cell body of the confluent astrocyte condition compared with the astrocyte free or sporadic astrocyte (Fig. 4). At points both more distal and more proximal to the cell body, there is no significant difference among the different conditions. This suggests the neurons in different astrocyte conditions differ mostly in the number of secondary and tertiary neurites rather than primary. As Table 1 shows, there was no significant difference among the three groups for neurite length, maximum intersecting radius, or critical radius.

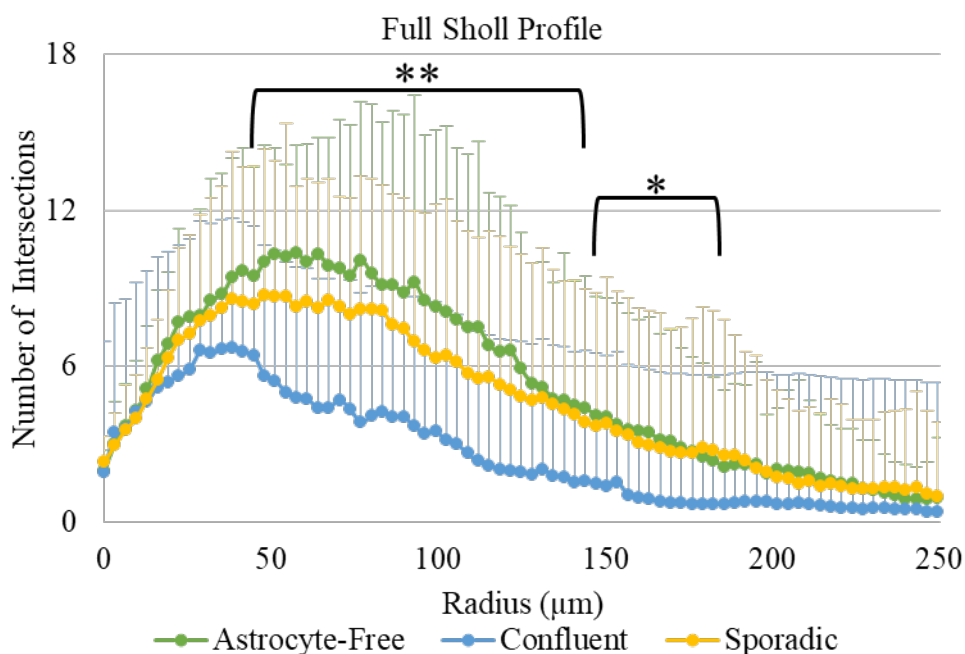


Fig. 4 Full Sholl profile graphing average number of intersections as function of distance from cell body for each astrocyte condition; neurons grown on confluent astrocytes had significantly less branching at 48–195 μm (48–145 μm , $**p < 0.01$; 145–195 μm , $*p < 0.05$)

4. Discussion

Three different ratios of astrocytes-to-neurons were successfully cultured from embryonic rat hippocampi. The cultures were characterized at DIV 12 to describe their cellular composition, cellular morphology, and neurite outgrowth. As expected, astrocyte-free cultures contained neurons but few to no astrocytes. In contrast, the confluent astrocyte cultures had a high astrocyte-to-neuron ratio, and sporadic astrocyte cultures had a relatively equal number of neurons and astrocytes intermingled together. Neurites from astrocyte free cultures did not appear as

healthy as their astrocyte-containing counterparts; the neurites appeared thinner with a punctate appearance along their lengths. While not quantified in this study, neurite thickness appeared to increase with the amount of astrocytes present in the culture: astrocyte free < sporadic astrocyte < confluent astrocyte. Furthermore, astrocyte free cultures were more likely to produce free-floating debris when compared with cultures containing astrocytes.

Astrocyte morphology was different among the two astrocyte-containing groups: the confluent astrocyte cultures presented as a fully connected layer of polygonal-shaped astrocytes similar to what others have described as the classical morphology.^{25,26} It is most likely the addition of serum in the confluent condition that is responsible for these differences. The astrocytes in the sporadic culture had defined processes extending outward from the cell body. Others have reported astrocytes of this morphology were indistinguishable from classical morphology in regard to functional and metabolic characteristics.²⁶

The healthy appearance of the neurons and neurites in the cultures containing astrocytes in this study is not surprising since astrocytes provide both functional and structural support to neurons. Functionally, astrocytes communicate with neurons to provide network regulation and neuroprotection,²⁷⁻³⁰ which is important for neuronal health. Even in astrocyte-free cultures, adding media or serum that mimics an astrocytic environment improves the health of neurons in culture.^{15,31,32} Structurally, astrocytes provide a more compliant environment on which neurons prefer to attach both *in vivo* and *in vitro*; having the astrocytes present in the culture will increase the attachment of neurons and quality of the culture compared with a glass cover slip alone.^{6,7}

While the inclusion of astrocytes is more representative of *in vivo* conditions, the actual ratio of astrocytes to neurons *in vivo* is still ambiguous.^{3,27,33,34} The ratio is influenced by the size of the brain, region examined, and the functional capacity of the animal species.³ In human brains, early studies suggested a 10:1 glia-to-neuron ratio, but 1:1 has been proposed more recently.^{3,27,34} In this study, the confluent (10:1) and sporadic (1:1) astrocyte conditions represent the published ratios for human brains, and the culture conditions can be selected based on the experimental needs. Although an astrocyte free condition does not represent any *in vivo* condition, an astrocyte free culture may be used to evaluate isolated neuronal responses without the influence of other cell types.³⁵

The Sholl analysis demonstrated a reduction in neurite branching as the density of astrocytes increased. Neuronal growth patterns in culture can be affected by neighboring cells, media additives, and the incubation environment.³⁶⁻⁴¹ For example, mature astrocytes have been shown to inhibit neurite outgrowth compared

with immature astrocytes.⁴² This may explain the smallest amount of branching in the confluent astrocyte condition witnessed in this study. Interestingly, the number of intersections among all groups were indistinguishable from one another until about 50 μm , suggesting all neurons regardless of astrocyte presence had similar numbers of primary branches. The confluent astrocyte condition had significantly fewer branches from about 50 to 200 μm , suggesting there were fewer secondary and tertiary branches. This is possibly the result of increased communication/support between the neurons and surrounding astrocytes. In contrast, the astrocyte free condition had a trend toward an increased number of secondary and tertiary branches that may be influenced by the neurons seeking to increase the chances of receiving trophic support from more remote neighboring cells, or by the lack of astrocyte-associated inhibition.

Depending on the type of experiment and analysis required, each media condition has benefits and limitations. A bed of confluent astrocytes provides a supportive structure for neurons to grow; however, because of the large ratio of astrocytes to neurons, it is difficult to discern subtle fluctuations in neuron morphology due to obstruction in visualization.⁴³ Furthermore, the specific cause of any neuronal changes, either structural or functional, is confounded by the presence of astrocytes. Astrocyte free conditions may allow for single neuronal cell analysis without the complication of other cells being present; however, this does not mimic the *in vivo* milieu. Even without an insult or treatment, neurons from these cultures do not survive as long as neurons cultured with astrocytes. To overcome these challenges, some laboratories add astrocyte-conditioned media or a feeding layer of astrocytes suspended above the neuronal culture.^{15,31,32,44}

5. Conclusion

In vitro models using brain cells reduce some of the complexity and offer a high degree of experimental control compared with *in vivo* experiments. Increased complexity better mimics the *in vivo* environment, but it is more difficult to resolve subtle effects. In this study, primary pyramidal neurons from hippocampi were cultured to obtain three configurations of varying complexity: confluent astrocyte—a layer of confluent astrocytes with neurons grown on top; sporadic astrocyte—neurons and astrocytes intermingled; and astrocyte free—neurons with no astrocytes present. This study describes the methodology to obtain these different neuronal-culture configurations and describes their neuronal environment, thereby providing a resource for researchers to choose the best neuron–astrocyte configuration for their intended research model.

6. References

1. Tsacopoulos M, Magistretti P. Metabolic coupling between glia and neurons. *J Neurosci.* 1996;163(3):8.
2. Edelman DB, Keefer EW. A cultural renaissance: in vitro cell biology embraces three-dimensional context. *Exp Neurol.* 2005;192(1):1–6.
3. Herculano-Houzel S. The glia/neuron ratio: how it varies uniformly across brain structures and species and what that means for brain physiology and evolution. *Glia.* 2014;62(9):1377–1391.
4. Araque A, Navarrete M. Glial cells in neuronal network function. *Philos Trans R Soc Lond B Biol Sci.* 2010;365(1551):2375–2381.
5. Sofroniew MV. Reactive astrocytes in neural repair and protection. *Neuroscientist.* 2005;11:400.
6. Lu YB, Franze K, Seifert G, Steinhauser C, Kirchhoff F, Wolburg H, Guck J, Janmey P, Wei EQ, Käs J, et al. Viscoelastic properties of individual glial cells and neurons in the CNS. *Proc Natl Acad Sci U S A.* 2006;103(47):17759–17764.
7. Miller WJ, Leventha I, Scarsella D, Haydon PG, Janmey P, Meaney DF. Mechanically induced reactive gliosis causes ATP-mediated alterations in astrocyte stiffness. *J Neurotrauma.* 2009;26:789–797.
8. Katayama Y, Maeda T, Koshinaga M, Kawamata T, Tsubokawa T. Role of excitatory amino acid-mediated ionic fluxes in traumatic brain injury. *Brain Pathol.* 1995;5(4):427–435.
9. Seidler NW, Jona I, Vegh M, Martonosi A. Cyclopiazonic acid is a specific inhibitor of the Ca²⁺-ATPase of sarcoplasmic reticulum. *J Biol Chem.* 1989;264(30):17816–17823.
10. Floyd CL, Rzigalinski BA, Weber JT, Sitterding HA, Willoughby KA, Ellis EF. Traumatic injury of cultured astrocytes alters inositol (1,4,5)-trisphosphate-mediated signaling. *Glia.* 2001;33(1):12–23.
11. Pekny M, Nilsson M. Astrocyte activation and reactive gliosis. *Glia.* 2005;50(4):427–434.
12. Morrison B 3rd, Saatman KE, Meaney DF, McIntosh TK. In vitro central nervous system models of mechanically induced trauma. *J Neurotrauma.* 1998;15.

13. Banker GA. Trophic interactions between astroglial cells and hippocampal neurons in culture. *Science*. 1980;209(4458):809–810.
14. Boehler MD, Wheeler BC, Brewer GJ. Added astroglia promote greater synapse density and higher activity in neuronal networks. *Neuron Glia Biol*. 2007;3(2):127–140.
15. Aebersold MJ, Thompson-Steckel G, Joutang A, Schneider M, Burchert C, Forro C, Weydert S, Han H, Vörös J. Simple and inexpensive paper-based astrocyte co-culture to improve survival of low-density neuronal networks. *Front Neurosci*. 2018;12:94.
16. Wanner IB, Deik A, Torres M, Rosendahl A, Neary JT, Lemmon VP, Bixby JL. A new in vitro model of the glial scar inhibits axon growth. *Glia*. 2008;56(15):1691–1709.
17. Bartlett WP, Banker GA. An electron microscopic study of the development of axons and dendrites by hippocampal neurons in culture. I. Cells which develop without intercellular contacts. *J Neuroscience*. 1984;4(8):1944–1953.
18. Bjorklund U, Persson M, Ronnback L, Hansson E. Primary cultures from cerebral cortex and hippocampus enriched in glutamatergic and GABAergic neurons. *Neurochem Res*. 2010;35(11):1733–1742.
19. Hansson E, Thorlin T. Brain primary cultures and vibrodissociated cells as tools for the study of astroglial properties and functions. *Dev Neurosci*. 1999;21(1):1–11.
20. Schindelin J, Arganda-Carreras I, Frise E, Kaynig V, Longair M, Pietzsch T, Preibisch S, Rueden C, Saalfeld S, Schmid B, et al. Fiji: an open-source platform for biological-image analysis. *Nat Methods*. 2012;9(7):676.
21. Longair M, Baker D, Armstrong J. Simple Neurite Tracer: open source software for reconstruction, visualization and analysis of neuronal processes. *Bioinformatics*. 2011;27(17):2453–2454.
22. Sholl DA. Dendritic organization in the neurons of the visual and motor cortices of the cat. *J Anat*. 1953;87(4):387.
23. Binley KE, Ng WS, Tribble JR, Song B, Morgan JE. Sholl analysis: a quantitative comparison of semi-automated methods. *J Neurosci methods*. 2014;225:65–70.
24. Langhammer CG, Previterra ML, Sweet ES, Sran SS, Chen M, Firestein BL. Automated Sholl analysis of digitized neuronal morphology at multiple scales:

- whole cell Sholl analysis versus Sholl analysis of arbor subregions. *Cytometry Part A*. 2010;77(12):116–118.
25. Souza DG, Bellaver B, Souza DO, Quincozes-Santos A. Characterization of adult rat astrocyte cultures. *PloS one*. 2013;8(3):e60282.
 26. Skytt DM, Madsen KK, Pajęcka K, Schousboe A, Waagepetersen HS. Characterization of primary and secondary cultures of astrocytes prepared from mouse cerebral cortex. *Neurochem Res*. 2010;35(12):2043–2052.
 27. Stevens B. Glia: much more than the neuron's side-kick. *Curr Biol*. 2003;13(12):R469–R472.
 28. Fields RD, Stevens-Graham B. New insights into neuron-glia communication. *Science*. 2002;298(5593):556–562.
 29. DiLeonardi AM, Matheis EA, Rafaels KA. The influence of glia on neuronal injury following mechanical loading in vitro. *J Neurotrauma*. 2018;35:A-2–A-285.
 30. Bambrick L, Kristian T, Fiskum G. Astrocyte mitochondrial mechanisms of ischemic brain injury and neuroprotection. *Neurochem Res*. 2004;29(3):601–608.
 31. Kaech S, Banker G. Culturing hippocampal neurons. *Nat Protoc*. 2006;1(5):2406–2415.
 32. Mahesh VB, Dhandapani KM, Brann DW. Role of astrocytes in reproduction and neuroprotection. *Mol Cell Endocrin*. 2006;246(1–2):1–9.
 33. Herculano-Houzel S, Collins CE, Wong P, Kaas JH. Cellular scaling rules for primate brains. *PNAS*. 2007;104(9):3562–3567.
 34. Hilgetag CC, Barbas H. Are there ten times more glia than neurons in the brain? *Brain Struct Funct*. 2009;213(4):365–366.
 35. Leong SY, Kaplan A, Wang LC, Almazan G, Fournier AE, Antel J. Properties of human central nervous system neurons in a glia-depleted (isolated) culture system. *J Neurosci Meth*. 2015;253:142–150.
 36. Chen H, Constantini S, Chen Y. Frontiers in neuroengineering a two-model approach to investigate the mechanisms underlying blast-induced traumatic brain injury. In: Kobeissy FH, editor. *Brain neurotrauma: molecular, neuropsychological, and rehabilitation aspects*. Boca Raton (FL): CRC Press/Taylor & Francis; 2015.

37. Chen L, Li W, Maybeck V, Offenhäusser A, Krause HJ. Statistical study of biomechanics of living brain cells during growth and maturation on artificial substrates. *Biomaterials*. 2016;106:240–249.
38. Treubert U, Brümmendorf T. Functional cooperation of β 1-integrins and members of the Ig superfamily in neurite outgrowth induction. *J Neurosci*. 1998;18(5):1795–1805.
39. Trinh-Trang-Tan MM, Bigot S, Picot J, Lecomte MC, Kordeli E. AlphaII-spectrin participates in the surface expression of cell adhesion molecule L1 and neurite outgrowth. *Exp Cell Res*. 2014;322(2):365–380.
40. McKeon RJ, Schreiber RC, Rudge JS, Silver J. Reduction of neurite outgrowth in a model of glial scarring following CNS injury is correlated with the expression of inhibitory molecules on reactive astrocytes. *J Neurosci*. 1991;11(11):3398–3411.
41. Brewer GJ, Torricelli J, Evege E, Price P. Optimized survival of hippocampal neurons in B27-supplemented Neurobasal™, a new serum-free medium combination. *J Neuroscience Res*. 1993;35(5):567–576.
42. Smith GM, Rutishauser U, Silver J, Miller RH. Maturation of astrocytes in vitro alters the extent and molecular basis of neurite outgrowth. *Dev Biol*. 1990;138(2):377–390.
43. Seibenhener ML, Wooten MW. Isolation and culture of hippocampal neurons from prenatal mice. *J Vis Exp*. 2012(65).
44. Zhu ZH, Yang R, Fu X, Wang YQ, Wu GC. Astrocyte-conditioned medium protecting hippocampal neurons in primary cultures against corticosterone-induced damages via PI3-K/Akt signal pathway. *Brain Res*. 2006;1114(1):1–10.

List of Symbols, Abbreviations, and Acronyms

2-D	2-dimensional
3-D	3-dimensional
ANOVA	analysis of variance
ARL	Army Research Laboratory
BSC	biosafety cabinet
CCDC	US Army Combat Capabilities Development Command
CNS	central nervous system
DAPI	4',6-diamidino-2-phenylindole
DIV	days in vitro
FBS	fetal bovine serum
GFAP	glial fibrillary acidic protein
HEB	Hibernate EB
NBM	neurobasal media
PBS	phosphate-buffered saline
PLL	poly-L-Lysine

1 DEFENSE TECHNICAL
(PDF) INFORMATION CTR
DTIC OCA

1 CCDC ARL
(PDF) FCDD RLD CL
TECH LIB

1 NORTSHORE UNIVERSITY HEALTH SYSTEM
(PDF) J FINAN

1 UNIFORMED SERVICES UNIVERSITY
(PDF) M SHAUGHNESS

2 MRMC DOD BLAST INJURY RSRCH
(PDF) PROG COORDINATING OFC
R SHOGE
T PIEHLER

15 CCDC ARL
(PDF) FCDD RLW L
AM DILEONARDI
T SHEPPARD
T THOMAS
C GOOD
A WEGENER
A DAGRO
A EIDSMORE
FCDD RLW
A RAWLETT
S SCHOENFELD
J ZABINSKI
A WEST
FCDD RLW PB
C HOPPEL
M KLEINBERGER
E MATHEIS
K RAFAELS